

1 **Direct detection of alpha satellite DNA with single-base resolution by**
2 **using abasic Peptide Nucleic Acids and Fluorescent *In Situ***
3 **Hybridization**

4 Agustín Robles-Remacho^{1,2,3}, M. Angélica Luque-González^{1,2,3}, F. Javier Lopez-
5 Delgado⁴, Juan J. Guardia-Monteagudo⁴, Mario Antonio Fara⁴, Salvatore Pernagallo⁴,
6 Rosario M. Sánchez-Martín^{*1,2,3}, Juan José Díaz-Mochón^{*1,2,3}

7 ¹GENYO. Centre for Genomics and Oncological Research: Pfizer / University of Granada / Andalusian
8 Regional Government. PTS Granada. Avenida de la Ilustracion, 114. 18016 Granada, Spain.

9
10 ²Department of Medicinal and Organic Chemistry, School of Pharmacy, University of Granada, Campus
11 Cartuja s/n, 18071 Granada, Spain.

12
13 ³Biosanitary Research Institute of Granada (ibs.GRANADA), University Hospital of Granada/University
14 of Granada, Avenida del Conocimiento, s/n, 18016 Granada, Spain.

15
16 ⁴DESTINA Genomica S.L. PTS Granada, Avenida de la Innovación 1, Edificio BIC, 18100 Armilla,
17 Granada, Spain

18
19 *Corresponding authors: Rosario M. Sánchez-Martín (rmsanchez@go.ugr.es) and Juan J. Díaz-Mochón
20 (juanjose.diaz@genyo.es).

21
22 **Abstract**

23 The detection of repetitive sequences with single-base resolution is becoming
24 increasingly important aiming to understand the biological implications of genomic
25 variation in these sequences. However, there is a lack of techniques to experimentally
26 validate sequencing data from repetitive sequences obtained by Next-Generation
27 Sequencing methods, especially in the case of Single-Nucleotide Variations (SNVs).
28 That is one of the reasons why repetitive sequences have been poorly studied and
29 excluded from most genomic studies. Therefore, in addition to sequencing data, there is
30 an urgent need for efficient validation methods of genomic variation in these sequences.
31 Herein we report the development of ChemFISH, an alternative method for the
32 detection of SNVs in repetitive sequences. ChemFISH is an innovative method based on
33 dynamic chemistry labelling and abasic Peptide Nucleic Acid (PNA) probes to detect *in*
34 *situ* the α -satellite DNA, organized in tandem repeats, with single-base resolution in a
35 direct and rapid reaction. With this approach, we detected by microscopy the α -satellite
36 DNA in a variety of human cell lines, we quantified the detection showing a low
37 coefficient of variation among samples (13.16 % - 25.33 %) and we detected single-

38 base specificity with high sensitivity (82.41 % - 88.82 %). These results indicate that
39 chemFISH can serve as a rapid method to validate previously detected SNVs in
40 sequencing data, as well as to find novel SNVs in repetitive sequences. Furthermore, the
41 versatile chemistry behind chemFISH can lead to develop novel molecular assays for
42 the *in situ* detection of nucleic acids.

43

44 **Graphical Abstract**

45

46

47 **Keywords**

48 Probe Chemistry; Peptide Nucleic Acids (PNAs); Fluorescent *in situ* Hybridization
49 (FISH); Repetitive sequences; Single-base resolution; Cell imaging

50

51

52

53 **1. Introduction**

54 The detection of nucleic acids preserving their spatial location in each individual
55 cell or tissue allows to establish precise molecular profiles. Most of the techniques for
56 such purpose are based on *in situ* hybridization (ISH), and, currently, some of these
57 techniques are being used to sequence *in situ* the detected nucleic acids [1–3]. That
58 results in a complete picture to understand the biological mechanisms involving these
59 nucleic acids. In the field of ISH techniques, Peptide Nucleic Acids (PNAs) have shown
60 their potential as efficient probes. These PNAs are analogues to DNA, where the sugar-
61 phosphate backbone is replaced by a peptide backbone formed by units of N-(1-
62 aminoethyl)-glycine [4,5]. Such modification results in probes with neutral charges with
63 a superior affinity to hybridize to their nucleic acids targets, forming more stable PNA-
64 DNA duplexes than the natural DNA or RNA duplexes [6]. PNAs have been mainly
65 used together with ISH techniques for the detection of repetitive sequences for
66 diagnostics purposes, such as centromeric and telomeric sequences, as well as ribosomal

67 RNA [7–10]. Moreover, the robustness using PNA probes has allowed to establish high-
68 throughput quantitative methods for a precise analysis of the detected targets [11,12].
69 However, the use of PNAs is restricted to the location of their targets, or a limited
70 discrimination among sequences by using a set of probes [13]. Then, the use of PNAs
71 does not allow to specifically identify single bases contained in the detected sequences.

72 One of the repetitive sequences detected by using PNA probes is the α -satellite
73 DNA. The α -satellite DNA constitutes the main component of centromeres and is
74 organized in long arrays of tandem DNA repeats [14,15]. These sequences represent the
75 ~3 % of the human genome and plays an important role in genomic stability [16]. The
76 α -satellite DNA is organized in multimeric High Order Repeats (HOR), each one
77 formed for the repetition of monomers of 171 bp-length [17]. The biological
78 implications of genomic variation in the sequence of the α -satellite DNA and other
79 repetitive sequences remain unclear. Different studies point that variability in the α -
80 satellite DNA, such as Single-Nucleotide Variations (SNVs), could have a major impact
81 on chromosomal functions and cell division [14,15,18]. However, the study of these
82 variability is limited. The reasons are that repetitive sequences have been poorly studied
83 and excluded from genomic assembly studies because they are not protein-coding
84 sequences [14,16] and, mainly, because over the past decade, Next-Generation
85 Sequencing methods have presented ambiguities in the assembly and interpretation of
86 single-base differences in the α -satellite DNA and other repetitive sequences [19–21].
87 Recently, a comprehensive study achieved a fully sequenced human genome, including
88 satellite repeats [22]. This great achievement will allow a better understanding of the
89 functions of these repetitive sequences. However, so far, there is a lack of techniques for
90 the detection of the α -satellite DNA with single-base resolution in a direct and rapid
91 manner. Such techniques could be a powerful tool for the validation of predicted SNVs
92 by sequencing data and computational analysis, as well as for the detection of novel
93 SNVs in repetitive sequences. These limitations urge to continue advancing for efficient
94 experimental validation methods of sequencing data and to improve the resolution
95 capabilities of ISH techniques, to achieve a better accuracy as well as to know details
96 about the sequence of the detected nucleic acids.

97 To address the limitation of detecting SNVs in repetitive sequences, in this
98 work, we report chemFISH, an innovative method for the detection of the human α -
99 satellite DNA with single-base resolution by microscopy. ChemFISH is a method based

100 on dynamic chemistry labelling and abasic PNA probes [23,24], and, with this
101 approach, we detected for the first time the α -satellite DNA *in situ*, as well as one
102 single base contained in its sequence, in a direct and rapid reaction. The abasic PNA
103 probes are chemically modified so that, in its strand, there is a nucleotide-free position
104 (known as abasic position) that lies opposite to a single base under study in the nucleic
105 acid target. When the abasic PNA hybridizes to its nucleic acid target, a chemical
106 pocket is formed with a secondary amine group opposite to that single base under study.
107 Then, aldehyde-modified nucleobases (called SMART-Nucleobases) [25] can be
108 incorporated in this abasic position. Following the Watson and Crick pairing rules, only
109 the complementary SMART-Nucleobase to the single base under study will react in the
110 chemical pocket, generating an iminium intermediate. Then, a reduction step lock-up
111 the SMART-Nucleobase as a stable tertiary amine in the complex. These SMART-
112 Nucleobases can be labelled with biomolecules or fluorophores, thus detecting the
113 specific SMART-Nucleobase incorporated to the chemical pocket and identifying the
114 single base under study. This approach based on dynamic chemistry labelling has been
115 previously implemented for the efficient detection of nucleic acids in liquid biopsy by
116 mass spectroscopy, flow cytometry, electrochemical and colorimetric analysis [26–30].

117 Using this approach, we detected the α -satellite DNA *in situ* with single-base
118 specificity, and, to assess the analytical performance, we explored the specific
119 incorporation of the SMART-Nucleobase, the reproducibility in different human cell
120 lines, and we performed a statistical analysis to know the consistency and robustness of
121 the reported method. The method reported here could be used as a tool to detect novel
122 SNVs in the human α -satellite DNA, as well as to validate SNVs predicted by
123 computational analysis. In addition, the chemistry developed in chemFISH is versatile
124 so that the abasic PNAs and the SMART-Nucleobases can be labelled with a range of
125 different labels and strategies [26–30].

126 **2. Materials and Methods**

127 **2.1. Design and synthesis of the abasic PNA probe**

128 The new PNA probe with the abasic position was designed 18-mer length and
129 complementary to a sequence present in the α -satellite DNA of all the centromeric
130 regions [31]. The PNA probe was designed labelled with Cy3-fluorophore and with the
131 abasic position in the central region, represented as *_* (N–Cy3–xx-

132 AAAC TAGA*_*_AGAAGCATT–C), where “xx” represents diethylene glycol
133 (miniPEG) as a spacer (for full details about the chemical structure and sequence of the
134 abasic PNA probe, see *Supporting Material 1*) The synthesis was carried out based on
135 standard solid phase synthesis techniques on polymeric supports (Tentagel resin
136 (Polymer, United Kingdom)) using an Intavis Bioanalytical MultiPrep CF synthesizer
137 (Intavis AG GmH, Germany). The synthesis was performed by repeated rounds of
138 coupling of activated PNA monomers with the amino group protected, followed by
139 deprotection of the terminal amino group with washing steps after each round. The
140 reactions were carried out at room temperature in microscale columns with a
141 polytetrafluoroethylene filter (Intavis, Germany). The abasic PNA probe and SMART-
142 Nucleobases were synthesized and characterized by DESTINA Genomica S.L. (Spain).

143 **2.2. Cell cultures**

144 All cell lines were provided by the Cell Bank of the Centre of Scientific
145 Instrumentation of Granada. The cell lines HT-29 (colorectal adenocarcinoma) (ECACC
146 91072201), MDA-MB-468 (mammary gland adenocarcinoma) (ATCC HTB-132),
147 HeLa (cervical adenocarcinoma) (ECACC 93021013) and MEF (*Mus musculus*)
148 (fibroblasts) (ATCC SCRC-1040) were grown in DMEM medium (Gibco, Paisley,
149 UK). The cell line H1975 (lung adenocarcinoma) (ATCC CRL-5908) was grown in
150 RPMI medium (Gibco, Paisley, UK). Both media were supplemented with 10 % fetal
151 bovine serum (Gibco, Paisley, UK), 100 U / mL penicillin / streptomycin (Gibco,
152 Paisley, UK), 1× L-glutamine (Gibco, Paisley, UK) and 1 mM sodium pyruvate (Sigma
153 Aldrich). The cell lines were grown at 37 °C in a 5% CO₂ humid incubator.

154 **2.3. Hypotonic shock**

155 Cell lines were grown in T25 flasks to 80 % confluence and trypsinized (1×
156 trypsin-EDTA solution, Sigma Aldrich) at 37 °C for 5 minutes. Then, cells were
157 collected and centrifuged for 5 minutes at 1500 rpm. The cell pellet was resuspended in
158 8 mL of hypotonic solution (0.075 M potassium chloride) and incubated at 37 °C for 30
159 minutes to obtain isolated nuclei. After this time, the nuclei were centrifuged for 5
160 minutes at 1500 rpm, the supernatant was removed and the fixative solution was added.

161 **2.4. Fixation**

162 The fixation was performed by slowly resuspending the cell pellet with a
163 fixative solution consisting in 1 part of glacial acetic acid to 3 parts of methanol. Then,
164 the sample was incubated for 30 minutes at 4 °C. The process was repeated 4 times and

165 then the nuclei were resuspended in 1 mL of fixative solution. Finally, two drops of the
166 suspension were added to a slide and airdried overnight. Up to 50 slides can be prepared
167 at once per each ~80 % confluent T25 flask. The slides that were not immediately used
168 for FISH, they were stored at 4 °C. When needed, the slides were blocked for one hour
169 with 3 % goat serum prior to the ChemFISH reaction.

170 **2.5. ChemFISH reaction**

171 Before hybridization, slides were immersed twice in PBS for two minutes and
172 then the samples were dehydrated by immersing the slides in increasing ethanol series
173 (70 % - 85 % - 100 %). Next, a chamber (Grace Bio-Labs, 9mm diameter, 0.8mm deep)
174 was strongly fixed to the slide, filled with PBS, and sealed. Next, denaturation was
175 carried out at 94 °C for 10 minutes in a Thermobrite (Abbott). After the denaturation,
176 the slides were placed in ice for 2 minutes. Then, the slides were removed from the ice
177 and the PBS was removed from the chamber. Next, the chamber was filled with the
178 hybridization solution. The hybridization solution consisted in 10 mM phosphate buffer
179 with pH carefully adjusted to 6, the abasic PNA probe at a final concentration of 50 nM,
180 the SMART-Cytosine-REX-PEG₁₂-Biotin (henceforth referred to as SMART-C-Biotin)
181 in a concentration of 5 μM and the reducing agent (NaBH₃CN) at a final concentration
182 of 1 mM and a final volume of 50 μL. Two control samples were running in the same
183 conditions, one without the SMART-C-biotin, and the other without the abasic PNA
184 probe. Once the hybridization solution was added, the chamber was sealed and placed in
185 a Thermobrite at 40 °C for 2 hours. After the incubation, the chamber was removed, and
186 the slides washed by immersion in SSC2 × 0.2 % Tween-20 or 5 minutes at 37 ° C.
187 Then, a second wash was performed by immersion in SSC2 × 0.1 % Tween-20 for 5
188 minutes followed by a water rinse, ready to proceed with the Tyramide Signal
189 Amplification (TSA).

190 **2.6. Tyramide Signal Amplification (TSA)**

191 The TSA reaction was performed following the manufacturer's instructions with
192 slight modifications (Tyramide SuperBoost™ kit with streptavidin and Alexa Fluor-
193 488, ThermoFisher Scientific). Briefly, three washes in PBS were performed for 10
194 minutes each, followed by one hr incubation with HRP-Peroxidase at room temperature
195 in a humid chamber. Then, another three washes in PBS were performed for 10 minutes
196 each. Next, the sample was incubated with 100 μL of working solution according to
197 manufacturer's instructions. The working solution contains the HRP-Peroxidase

198 substrate (tyramide conjugated with Alexa Fluor 488) and H₂O₂. The reaction was
199 incubated for 10 minutes. Next, the samples were rinsed three times with PBS and
200 nuclear staining was carried out, depositing 5 µL of mounting medium with DAPI (1.5
201 µg / mL) (Vectashield Antifade). Then, the sample was covered with a coverslip and
202 sealed. Slides were ready to be detected by confocal microscopy.

203 **2.7. Confocal microscopy**

204 Images used for quantification were obtained with a Zeiss LSM 710 inverted
205 confocal laser microscope with a 63× / 1.4, 1.0, 2.0 plan-apochromatic oil zoom factor.
206 The lasers used were 405 nm diode laser at 3.0 % for DAPI, argon laser 488 nm at 2.2
207 % for Alexa Fluor 488 and HeNe laser 543 nm at 10.0 % for Cy3. The acquisition was
208 performed sequentially, maintaining each filter individually configured to avoid
209 interference between channels. DAPI detection range: 410-487 nm; Alexa Fluor 488:
210 488-524 nm; Cy3: 543-618 nm.

211 **2.8. Specific incorporation of SMART-C-Biotin**

212 To determine the specific incorporation of SMART-C-Biotin, four independent
213 assays were carried out, each one with one of the four biotinylated SMART-
214 Nucleobases at 5 µM. The SMART-Nucleobases used were SMART-C-biotin,
215 SMART-Adenine-deaza-enol-PEG₁₂-biotin (henceforth referred to as SMART-A-
216 biotin), SMART-Guanine-deaza-enol-PEG₁₂-biotin (henceforth referred to as SMART-
217 G-biotin) and SMART-Thymine-REX-PEG₁₂-biotin (SMART-T-Biotin). Control
218 samples were run in the same conditions, but without the biotinylated SMART-
219 Nucleobase in each case. Reactions were performed in the same conditions above
220 detailed (section 2.5), followed by the TSA and visualized by confocal microscopy (as
221 described in section 2.7).

222 **2.9. Reproducibility and specific detection of human α-satellite DNA**

223 The method was initially developed in the human cell line HT-29, which is a
224 colorectal adenocarcinoma cell line and subsequently validated in the human cell lines
225 MDA-MB-468 (mammary gland adenocarcinoma), H1975 (lung adenocarcinoma) and
226 HeLa (cervical adenocarcinoma). To test the specific detection of α-satellite DNA of
227 human species, a test was carried out by using a mouse (*Mus musculus*) cell line of
228 fibroblasts, MEF. All reactions were performed in the same conditions above detailed
229 (section 2.5) and visualized by confocal microscopy (as described in section 2.7).

230 **2.10. Analytical performance and statistical analysis**

231 To determine the analytical performance of the reported method, a quantification
232 was carried out for both discrete signals: Cy3 (α -satellite DNA) and AF488 (single-base
233 detection) signals. For this purpose, the assay was repeated three times in three cell
234 lines, and then, 25 metaphase nuclei and 50 interphase nuclei were randomly imaged.
235 The quantification was performed using ImageJ software (NIH, USA) and the number
236 of discrete signals for both Cy3 and AF488 was averaged using GraphPad Prism
237 software. The average number of red and green signals were compared to the modal
238 number (number of chromosomes per nucleus) provided by ATCC (Manassas, VA,
239 USA) of each cell line. Coefficients of variation for each cell line were calculated.
240 Then, to know the sensitivity of single-base resolution, we compared both averaged
241 discrete signals in a ratio AF488: Cy3.

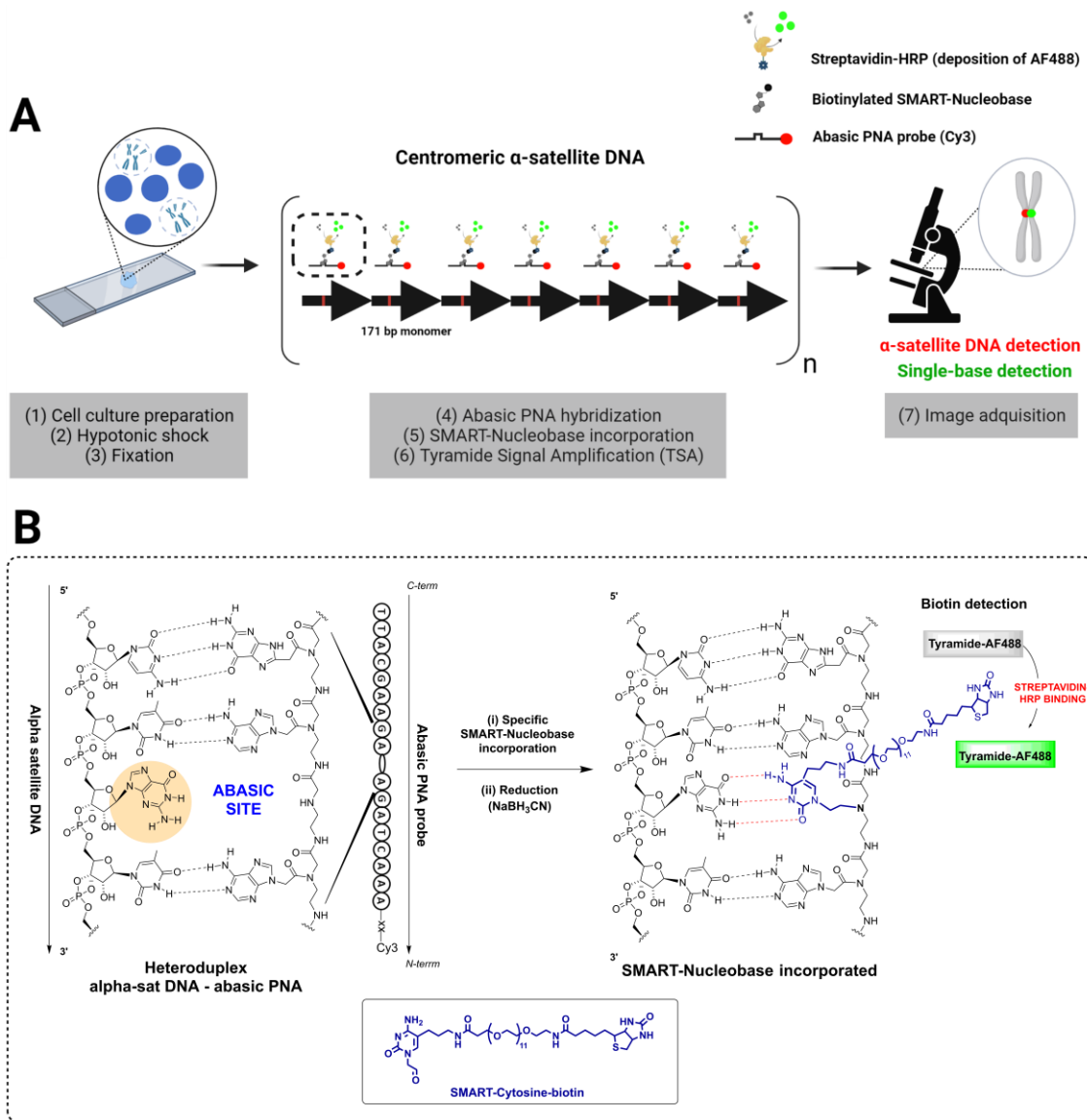
242 **3. Results and discussion**

243 **3.1. Detection of centromeric α -satellite DNA with single-base resolution by** 244 **chemFISH**

245 To assess the use of chemFISH, we carried out a proof of principle to detect the
246 α -satellite DNA *in situ* with single-base specificity in the human colorectal
247 adenocarcinoma cell line HT-29. We designed an abasic PNA probe complementary to
248 a consensus sequence present in the 171-bp monomer of the human α -satellite DNA of
249 all centromeres [31]. This PNA probe has the abasic position in the central region,
250 represented as *_*, and Cy3-fluorophore labelling at the N-terminus (N-Cy3-xx-
251 AAACTAGA*_*AGAAGCATT-C). Therefore, due to the repetitive nature of
252 centromeres, the abasic PNA probe hybridizes in tandem staining all centromeres in red
253 (Cy3). Considering the consensus sequence of the α -satellite DNA, the abasic position
254 lied opposite to a guanine in each monomer, so we used a biotinylated aldehyde
255 modified Cytosine (SMART-C-biotin) to detect that guanine. After hybridization of the
256 abasic PNA probe, the SMART-C-biotin was incorporated to each abasic site and
257 chemically lock-up by reductive amination. After the reaction, we revealed the biotin
258 with Tyramide Signal Amplification (TSA), which deposits Alexa Fluor-488
259 fluorophores surrounding the reaction. Therefore, the single bases were detected as
260 green signals (AF488). Under the microscope, the co-localization of both signals

261 indicates the detection of the α -satellite DNA (Cy3) with single-base resolution
 262 (AF488). (**Figure 1**).

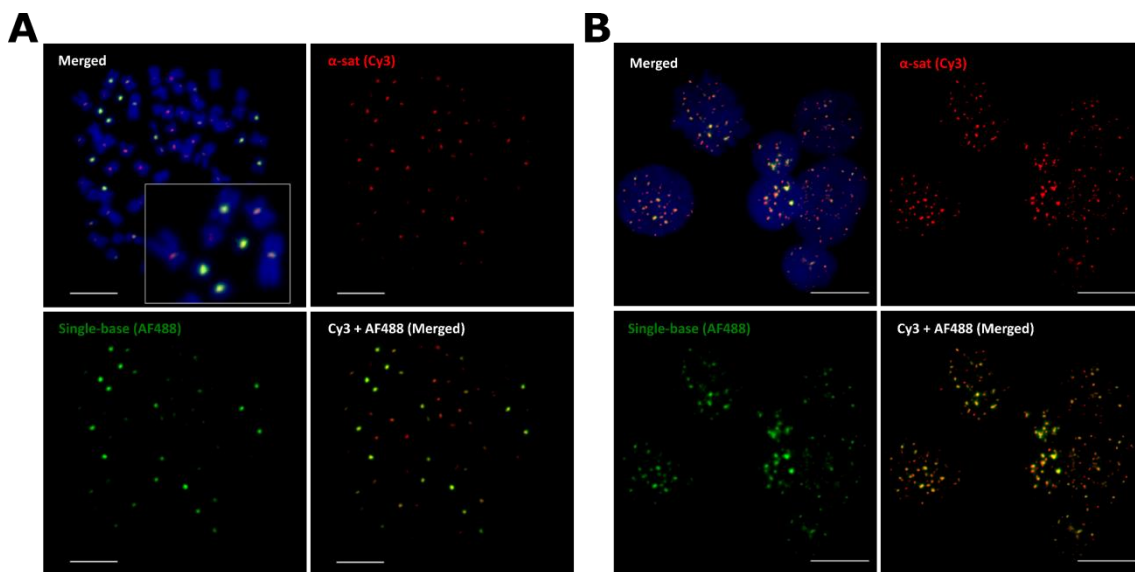
263



264

265 **Figure 1. Schematics of chemFISH reaction.** **A-** Schematics of full analytical protocol of chemFISH.
 266 Cell culture were grown, trypsinized and incubated with a hypotonic solution to obtain isolated nuclei.
 267 The isolated nuclei were fixated and deposited in slides. Then, chemFISH was carried out incubating the
 268 isolated nuclei with the abasic PNA probe (Cy3-labelled) and the SMART-Nucleobase (biotin-labelled).
 269 After the reaction, the biotin was revealed with Tyramide Signal Amplification (TSA), what deposits
 270 tyramide-Alexa Fluor 488 surroundings the reaction. Under the microscope, red signals (Cy3) were
 271 indicative of the α -satellite DNA detection while green signals (AF488) were indicative of single-base
 272 detection. **B-** Chemical details of chemFISH reaction. The abasic PNA probe (Cy3-labelled) hybridized a
 273 sequence in the α -satellite DNA and the abasic position lied in front of a single base under study
 274 (highlighted in red). Then, the complementary SMART-Nucleobase (biotin-labelled) was incorporated in
 275 the abasic position. The reaction was lock-up by a reductive amination and biotin revealed with TSA.

276 Obtained results showed that both signals co-localized in the centromere of
277 chromosomes in metaphase nuclei (**Figure 2**). However, in interphase nuclei both co-
278 localized signals were dispersed, due to the relaxed nature of chromatin. Notably, when
279 the sample were running without the SMART-C-biotin as negative control, no signals
280 were found in AF488 channel. In addition, when the sample was running without the
281 abasic PNA probe, no signals were found in Cy3 or AF488 channels. Our results
282 indicated that we detected successfully a sequence contained in the 171-bp monomer of
283 the α -satellite DNA and a guanine in a specific position in this sequence. Remarkably,
284 this method has been optimised to be done in less than 6 hrs using standard materials
285 and reagents for microscopy analysis. Moreover, we performed a benchmarking of
286 ChemFISH with two commercial probes for PNA-FISH, showing a similar detection of
287 the α -satellite DNA with the advantage that ChemFISH allows the specific detection of
288 a single base. All these data are presented in *Supporting Material 2*.



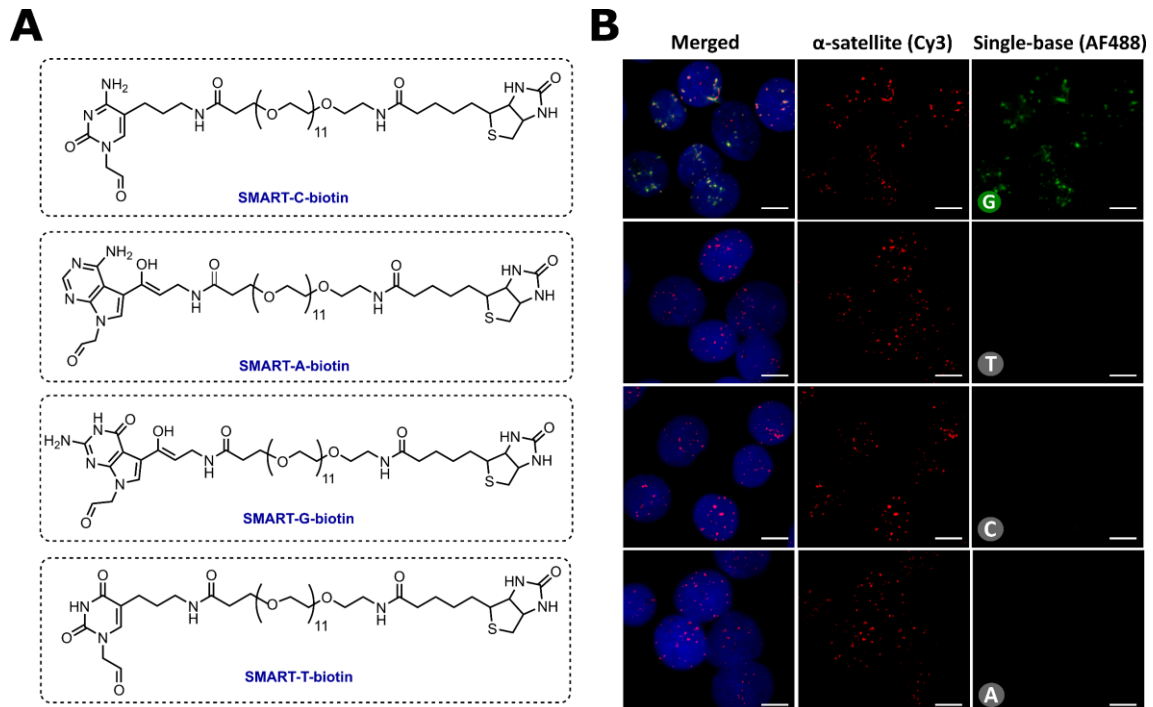
289

290 **Figure 2. ChemFISH for the detection of the α -satellite DNA (Cy3) with single-base resolution**
291 **(AF488) in the centromere of metaphase (A) and interphase nuclei (B).** A- Cy3 and AF488 discrete
292 signals co-localized in the centromere of metaphase nuclei. B- Cy3 and AF488 discrete signals co-
293 localized dispersed in interphase nuclei. Cell line: HT-29. Images obtained by inverted confocal
294 microscopy (Zeiss LSM 710). 63x magnification. Zoom factor (A): 2.0. Zoom factor (B): 1.5. Scale bar
295 (A): 10 μ m. Scale bar (B): 20 μ m

296 3.2. Specific incorporation of SMART-C-Biotin

297 To determine the specific detection of guanine, we carried out four independent
298 assays using the abasic PNA probe under the same conditions but shifting the SMART-
299 Nucleobase used in each assay. For each assay we used a different biotinylated

300 SMART-Nucleobase (SMART-C-biotin, SMART-A-biotin, SMART-G-biotin and
301 SMART-T-biotin). The results showed green signals (AF488) only when the SMART-
302 C-biotin was used, so indicating the detection of a guanine (**Figure 3**).



303

304 **Figure 3. Specific incorporation of SMART-C-biotin, detecting a guanine (AF488).** A- Four different
305 biotinylated SMART-Nucleobases were tested. B- Only when SMART-C-Biotin was used, there was
306 signals in the AF488 channel, therefore, detecting a guanine in the α -satellite DNA. Cell line: HT-29.
307 Images obtained by inverted confocal microscopy (Zeiss LSM 710). 63x magnification. Zoom factor 1.5.
308 Scale bar: 10 μ m.

309 This result prove that a guanine is the predominant nucleobase in that position
310 reinforcing the single-base specificity of this method. As we did not find green signals
311 using other biotinylated SMART-Nucleobases, we concluded that there were no high-
312 frequency polymorphisms in this position. With this approach, we detected the α -
313 satellite DNA and a single base contained in its sequence by using a unique abasic PNA
314 probe, in contrast with the approach of using a set of PNA probes, which is limited to
315 thermal hybridization differences among the probes and does not detect specifically a
316 single base [12,31].

317 With the aim to test the cross-reactivity between the four biotinylated SMART-
318 Nucleobases, we carried out a mass spectrometry analysis by using MALDI-TOF. The
319 mass spectra showed that only the complementary SMART-Nucleobase can be
320 incorporated to the abasic site, thus, detecting specifically the nucleobase under study.
321 These data showed the specificity of the method lacking cross-reactivity between the

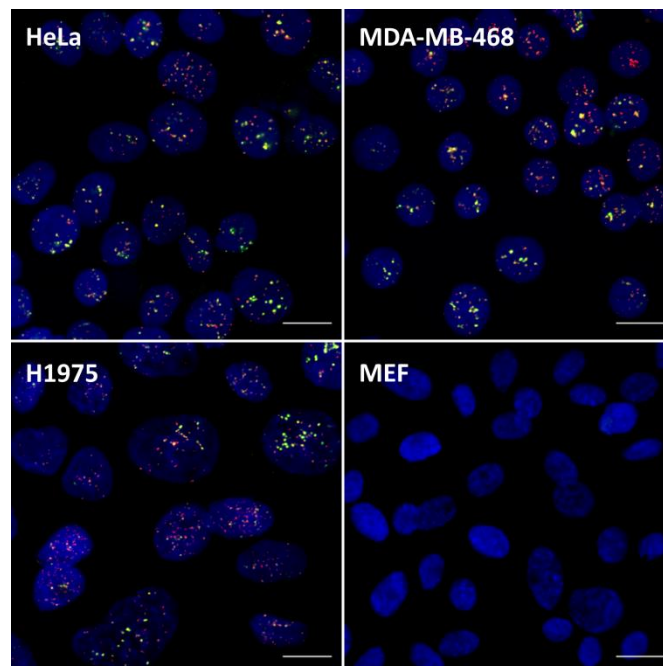
322 biotinylated SMART-Nucleobases. All these data can be found in *Supporting Material*
323 3.

324

325

326 3.3. Reproducibility and specific detection of human α -satellite DNA

327 In order to evaluate the versatility of this approach, we extended the method to
328 the human cell lines MDA-MB-468 (mammary gland adenocarcinoma), H1975 (lung
329 adenocarcinoma) and HeLa (cervical adenocarcinoma). We detected in all cases the
330 human α -satellite DNA with single-base resolution, detecting guanine (**Figure 4**). The
331 abasic PNA probe used in our experiments is specific for human species, so, to
332 determine the absence of non-specificity bindings to other centromeric regions of other
333 species, we used a mouse (*Mus musculus*) cell line, MEF (fibroblasts). The results
334 showed no detection of the α -satellite DNA or single-bases in the mouse cell line
335 (Figure 4). To see the full images obtained in each individual channel using different
336 cell lines, see *Supporting Material 4*. These results indicated that the method can be
337 applied to different human cell lines. Also, these results indicated that the abasic PNA
338 probe is specific of humans, as there were not non-specific signals of centromeric
339 sequences of other species different to humans.



340

341 **Figure 4. ChemFISH reaction in different human cell lines and a mouse cell line.** The human α -
342 satellite DNA (Cy3 signals) with single-base resolution (AF488 signals) was detected in different human

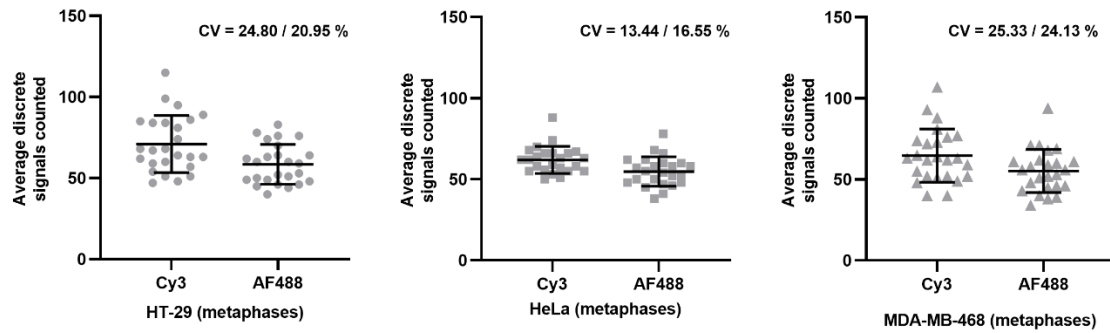
343 cell lines (HeLa, MDA-MB-468, H1975). There was no detection in the mouse cell line (MEF). All
344 channel merged. Images obtained by inverted confocal microscopy (Zeiss LSM 710). 63x magnification.
345 Scale bar: 20 μm .

346 **3.4. Analytical performance and statistical analysis**

347 To assess the analytical performance of this method, we performed a statistical
348 analysis. For that purpose, a quantification was carried out for both discrete signals: Cy3
349 (α -satellite DNA) and AF488 (guanine detection). The assay was repeated three times in
350 the cell lines HT-29, HeLa and MDA-MB-468, and then, 25 metaphase nuclei were
351 randomly imaged in each cell line. The quantification was performed using ImageJ
352 software (NIH, USA) and the number of discrete signals for both Cy3 and AF488 was
353 averaged as red (Cy3) or green (AF488) signals per nucleus. In order to know the
354 sensitivity of single-base detection, we established the AF488: Cy3 ratio, that indicates
355 the percentage of guanine detected in the position under study per each α -satellite DNA
356 sequence detected. To establish the ratio, we used the average number of green and red
357 signals per nucleus in each cell line. We successfully detected a guanine in a range of 82
358 % to 89 % of all detected α -satellite DNA. Also, we calculated the coefficients of
359 variation for both signals. Coefficients of variation for red signals were 24.80 % (HT-
360 29) 13.16 % (HeLa), and 25.33 % (MDA-MB-468). Coefficients of variation for green
361 signals were 20.95% (HT-29), 16.29 % (HeLa), and 24.13 % (MDA-MB-468). These
362 data showed a low variability detecting the α -satellite DNA with single-base resolution
363 among samples.

364 As the method stains all centromeres, we expected to detect one discrete Cy3
365 and AF488 signal per centromere per chromosome. Thus, we compared the average
366 number of Cy3 and AF488 discrete signals per nucleus with the modal number (number
367 of chromosomes per nucleus) provided by different references [33–35]. We detected the
368 average of Cy3 discrete signals (α -satellite DNA) in a consistent range compared with
369 the modal number of other references. Consistently with the sensitivity for guanine
370 detection, the average of AF488 discrete signals was in a lower range to the modal
371 number in all cell lines (**Figure 5**). Individual data of the average of discrete signals,
372 coefficients of variation and performance ratio are represented in **Table 1**.

373



374

375 **Figure 5. Comparison of the average number of Cy3 discrete signals (α -satellite DNA) and AF488**
 376 **discrete signals (single-base detection) detected per nucleus in 25 metaphase nuclei of different cell**
 377 **lines. Coefficient of variation (CV) is represented in the graphics as CV = % CV Cy3 discrete signals / %**
 378 **CV AF488 discrete signals.**

379

380 **Table 1. Statistical analysis of the quantification of the signal obtained from the α -satellite DNA**
 381 **(Cy3) detection and the single-base (AF488) detection in 25 metaphase nuclei of different cell lines.**
 382 **The average of discrete Cy3 or AF488 signals is represented as mean \pm SD.**

Cell line (25 metaphase nuclei)	HT-29	HeLa	MDA-MB-468
Average of Cy3 discrete signals (red)	70.96 \pm 17.60	61.92 \pm 8.149	64.72 \pm 16.39
Coefficient of variation of Cy3 discrete signals (red)	24.80 %	13.16 %	25.33 %
Average of AF488 discrete signals (green)	58.48 \pm 12.25	55.00 \pm 8.958	55.24 \pm 13.33
Coefficient of variation of AF488 discrete signals	20.95 %	16.29 %	24.13 %
Performance: Ratio AF488: Cy3	82.41 %	88.82 %	85.35 %
Modal number according to references	68-72 [33]	Aneuploid [34]	60-67 [35]

383

384 In addition, we performed a statistical analysis in interphase nuclei. For this end,
 385 the assay was repeated three times for each cell line, and then, we increased the number
 386 of interphase nuclei randomly imaged to 50 in each cell line. The reason for that
 387 increase is that in interphase nuclei the chromatin is relaxed, and single centromeres can
 388 be difficult to identify, due to different centromeric regions being near each other and
 389 generating one single discrete signal. Consistently with this reasoning, we found a lower
 390 average number of Cy3 and AF488 discrete signals for each cell line compared to the

391 modal number and the coefficients of variation was high among samples. The full
392 statistical analysis of the average of discrete signals, coefficients of variation and
393 performance ratio for each discrete signal in interphase nuclei can be found in
394 *Supporting Material 5*.

395 The statistical analysis showed that chemFISH is consistent analysing discrete
396 signals in metaphase nuclei, with reproducibility among samples and different human
397 cell lines. We found low variability when analysing metaphase nuclei, and we
398 successfully detected single bases in the 85.52 % of the detected α -satellite DNA
399 sequences. This result remark the novelty of the sensitive detection of the α -satellite
400 DNA with single-base resolution in a direct and rapid assay while maintaining its spatial
401 location.

402 **4. Conclusions**

403 Here, we report the development of chemFISH, an innovative method to detect *in*
404 *situ* the α -satellite DNA with single-base resolution in a direct and rapid reaction.
405 ChemFISH is a method based on dynamic chemistry labelling and abasic PNA probes.
406 We detected by microscopy the α -satellite DNA with single-resolution in different
407 human cell lines, showing reproducibility in different human cell lines and specificity to
408 human species. We analysed the absence of cross-reactivity between the four
409 biotinylated SMART-Nucleobases, showing specificity. We tested the analytical
410 performance, finding a low variability (coefficients of variation ranging from 13.16 %
411 to 25.33 %) and we detected single bases with high sensitivity (we detected single-base
412 specificity in a range from 82.41 % to 88.82 % of all detected α -satellite DNA). The
413 method and the analysis can be carried out in less than 6 hrs, using standard materials
414 and reagents for microscopy analysis.

415 ChemFISH is a promising method that can serve to validate previously predicted
416 SNVs by sequencing data and computational analysis, as well as to find novel SNVs in
417 repetitive sequences. The molecular development is compatible to detect other repetitive
418 sequences typically detected by using PNAs and ISH techniques, such as telomeric
419 sequences and ribosomal RNAs [7–10]. The method is limited to the detection of
420 abundant nucleic acids, however, as future approaches, the method could be compatible
421 to detect transcripts as well, as there are ISH techniques based in an isothermal
422 amplification to generate artificial repetitive sequences around the transcripts, facilizing

423 their detection [1,36]. In addition, the chemistry behind chemFISH is versatile as the
424 abasic PNA probe as well as the SMART-Nucleobases could be labelled and conjugated
425 to different type of biomolecules and fluorophores, as previous studies have shown [26–
426 30]. In conclusion, the method presented here could contribute to the development of
427 novel molecular assays based on PNA and ISH techniques to detect abundant nucleic
428 acids *in situ*, as well as information contained in their sequences.

429 **Acknowledgments**

430 This research was supported by the Spanish Ministry of Economy and Competitiveness
431 (grant number BIO2016-80519-R, PID2019.110987RB.I00); the Andalusian Regional
432 Government-FEDER (PT18-TP-4160, B-FQM-475-UGR18, A-FQM-760-UGR20); the
433 European Union’s Horizon 2020 research and innovation program under the Marie
434 Skłodowska-Curie actions (MSCA-RISE-101007934). The authors are members of the
435 NANOCARE network (RED2018-102469-T) funded by the State Investigation Agency.
436 ARR thanks the Spanish Ministry of Education for PhD funding
437 (scholarship FPU15/06418) and the University of Granada for postdoctoral research. FJ
438 López-Delgado thanks the Spanish Ministry of Economy and Competitiveness for the
439 Torres Quevedo fellowship (PTQ-16-08597). These studies were approved and
440 supported by DESTINA Genomics Ltd. Schemes in Graphical abstract and Fig. 1 have
441 been partially created using BioRender.com. We thank Raquel Marrero-Díaz for her
442 valuable support in the microscopy analyses.

443 **References**

- 444 [1] R. Ke, M. Mignardi, A. Pacureanu, J. Svedlund, J. Botling, C. Wählby, M. Nilsson, In
445 situ sequencing for RNA analysis in preserved tissue and cells, *Nat. Methods*. 10 (2013)
446 857–860. <https://doi.org/10.1038/nmeth.2563>.
- 447 [2] A.C. Payne, Z.D. Chiang, P.L. Reginato, S.M. Mangiameli, E.M. Murray, C.-C. Yao, S.
448 Markoulaki, A.S. Earl, A.S. Labade, R. Jaenisch, G.M. Church, E.S. Boyden, J.D.
449 Buenrostro, F. Chen, In situ genome sequencing resolves DNA sequence and structure in
450 intact biological samples., *Science*. 908 (2020). <https://doi.org/10.1126/science.aay3446>.
- 451 [3] M. Asp, J. Bergenstråhle, J. Lundeberg, Spatially Resolved Transcriptomes—Next
452 Generation Tools for Tissue Exploration, *BioEssays*. 42 (2020).
453 <https://doi.org/10.1002/bies.201900221>.

- 454 [4] J. Saarbach, P.M. Sabale, N. Winssinger, Peptide nucleic acid (PNA) and its applications
455 in chemical biology, diagnostics, and therapeutics, *Curr. Opin. Chem. Biol.* 52 (2019)
456 112–124. <https://doi.org/10.1016/j.cbpa.2019.06.006>.
- 457 [5] A. Gupta, A. Mishra, N. Puri, Peptide nucleic acids: Advanced tools for biomedical
458 applications, *J. Biotechnol.* 259 (2017) 148–159.
459 <https://doi.org/10.1016/j.jbiotec.2017.07.026>.
- 460 [6] P.E. Nielsen, M. Egholm, R.H. Berg, O. Buchardt, Sequence-Selective Recognition of
461 DNA by Strand Displacement with a Thymine- Substituted Polyamide Author (s): Peter
462 E . Nielsen , Michael Egholm , Rolf H . Berg and Ole Buchardt Published by : American
463 Association for the Advancement of Science Stable, *Science*. 254 (1991) 1497.
- 464 [7] H. Stender, B. Williams, J. Coull, PNA fluorescent in situ hybridization (FISH) for rapid
465 microbiology and cytogenetic analysis, *Methods Mol. Biol.* 1050 (2014) 167–178.
466 https://doi.org/10.1007/978-1-62703-553-8_14.
- 467 [8] F. Pellestor, P. Paulasova, S. Hamamah, Peptide Nucleic Acids (PNAs) as Diagnostic
468 Devices for Genetic and Cytogenetic Analysis, *Curr. Pharm. Des.* 14 (2008) 2439–2444.
469 <https://doi.org/10.2174/138161208785777405>.
- 470 [9] H. Stender, PNA FISH: An intelligent stain for rapid diagnosis of infectious diseases,
471 *Expert Rev. Mol. Diagn.* 3 (2003) 649–655. <https://doi.org/10.1586/14737159.3.5.649>.
- 472 [10] F. Pellestor, P. Paulasova, M. Macek, S. Hamamah, The use of peptide nucleic acids for
473 in situ identification of human chromosomes, *J. Histochem. Cytochem.* 53 (2005) 395–
474 400. <https://doi.org/10.1369/jhc.4R6399.2005>.
- 475 [11] P. Slijepcevic, Telomere length measurement by Q-FISH, *Methods Cell Sci.* 23 (2001)
476 17–22. <https://doi.org/10.1023/A:1013177128297>.
- 477 [12] A. Canela, E. Vera, P. Klatt, M.A. Blasco, High-throughput telomere length
478 quantification by FISH and its application to human population studies, *Proc. Natl.*
479 *Acad. Sci. U. S. A.* 104 (2007) 5300–5305. <https://doi.org/10.1073/pnas.0609367104>.
- 480 [13] B.S. Gaylord, M.R. Massie, S.C. Feinstein, G.C. Bazan, SNP detection using peptide
481 nucleic acid probes and conjugated polymers: Applications in neurodegenerative disease
482 identification, *Proc. Natl. Acad. Sci. U. S. A.* 102 (2005) 34–39.
483 <https://doi.org/10.1073/pnas.0407578101>.
- 484 [14] K.H. Miga, Y. Newton, M. Jain, N. Altemose, H.F. Willard, E.J. Kent, Centromere
485 reference models for human chromosomes X and y satellite arrays, *Genome Res.* 24
486 (2014) 697–707. <https://doi.org/10.1101/gr.159624.113>.

- 487 [15] M.E. Aldrup-MacDonald, M.E. Kuo, L.L. Sullivan, K. Chew, B.A. Sullivan, Genomic
488 variation within alpha satellite DNA influences centromere location on human
489 chromosomes with metastable epialleles, *Genome Res.* 26 (2016) 1301–1311.
490 <https://doi.org/10.1101/gr.206706.116>.
- 491 [16] K.H. Miga, The Promises and Challenges of Genomic Studies of Human Centromeres,
492 in: B.E. Black (Ed.), *Centromeres Kinetochores Discov. Mol. Mech. Underlying*
493 *Chromosom. Inherit.*, Springer International Publishing, Cham, 2017: pp. 285–304.
494 https://doi.org/10.1007/978-3-319-58592-5_12.
- 495 [17] B.A.S. Shannon M McNulty, Alpha satellite DNA biology: finding function in the
496 recesses of the genome, 2018. <https://doi.org/10.1007/s10577-018-9582-3>.
- 497 [18] V. Barra, D. Fachinetti, The dark side of centromeres: types, causes and consequences of
498 structural abnormalities implicating centromeric DNA, *Nat. Commun.* 9 (2018).
499 <https://doi.org/10.1038/s41467-018-06545-y>.
- 500 [19] K.H. Miga, I.A. Alexandrov, Variation and Evolution of Human Centromeres: A Field
501 Guide and Perspective, *Annu. Rev. Genet.* 55 (2021) 583–602.
502 <https://doi.org/10.1146/annurev-genet-071719-020519>.
- 503 [20] O.K. Tørresen, B. Star, P. Mier, M.A. Andrade-Navarro, A. Bateman, P. Jarnot, A.
504 Gruca, M. Grynberg, A. V. Kajava, V.J. Promponas, M. Anisimova, K.S. Jakobsen, D.
505 Linke, Tandem repeats lead to sequence assembly errors and impose multi-level
506 challenges for genome and protein databases, *Nucleic Acids Res.* 47 (2019) 10994–
507 11006. <https://doi.org/10.1093/nar/gkz841>.
- 508 [21] M. Cechova, Probably correct: Rescuing repeats with short and long reads, *Genes*
509 (Basel). 12 (2021) 1–13. <https://doi.org/10.3390/genes12010048>.
- 510 [22] S. Nurk, The complete sequence of a human genome, *Science* (80-.). 376 (2022) 44–53.
- 511 [23] F.R. Bowler, J.J. Diaz-Mochon, M.D. Swift, M. Bradley, DNA analysis by dynamic
512 chemistry, *Angew. Chemie - Int. Ed.* 49 (2010) 1809–1812.
513 <https://doi.org/10.1002/anie.200905699>.
- 514 [24] F.R. Bowler, P.A. Reid, C. Boyd, J.J. Diaz-Mochon, M. Bradley, Dynamic chemistry for
515 enzyme-free allele discrimination in genotyping by MALDI-TOF mass spectrometry,
516 *Anal. Methods.* 3 (2011) 1656–1663. <https://doi.org/10.1039/c1ay05176h>.
- 517 [25] M. Bradley; J.J. Díaz-Mochón, Nucleobase characterisation, (2014).
518 <https://doi.org/https://patents.google.com/patent/US8716457/en>.

- 519 [26] M. Angélica Luque-González, M. Tabraue-Chávez, B. López-Longarela, R. María
520 Sánchez-Martín, M. Ortiz-González, M. Soriano-Rodríguez, J. Antonio García-Salcedo,
521 S. Pernagallo, J. José Díaz-Mochón, Identification of Trypanosomatids by detecting
522 Single Nucleotide Fingerprints using DNA analysis by dynamic chemistry with MALDI-
523 ToF, *Talanta*. 176 (2018) 299–307. <https://doi.org/10.1016/j.talanta.2017.07.059>.
- 524 [27] A. Marín-Romero, A. Robles-Remacho, M. Tabraue-ChAvez, Ba. López-Longarela,
525 R.M. SAnchez-Martín, J.J. Guardia-Monteagudo, M.A. Fara, F.J. López-Delgado, S.
526 Pernagallo, J.J. Díaz-Mochón, A PCR-free technology to detect and quantify
527 microRNAs directly from human plasma, *Analyst*. 143 (2018) 5676–5682.
528 <https://doi.org/10.1039/c8an01397g>.
- 529 [28] A. Delgado-Gonzalez, A. Robles-Remacho, A. Marin-Romero, S. Detassis, B. Lopez-
530 Longarela, F.J. Lopez-Delgado, D. de Miguel-Perez, J.J. Guardia-Monteagudo, M.A.
531 Fara, M. Tabraue-Chavez, S. Pernagallo, R.M. Sanchez-Martin, J.J. Diaz-Mochon, PCR-
532 free and chemistry-based technology for miR-21 rapid detection directly from tumour
533 cells, *Talanta*. 200 (2019) 51–56. <https://doi.org/10.1016/j.talanta.2019.03.039>.
- 534 [29] M. Tabraue-Chávez, M.A. Luque-González, A. Marín-Romero, R.M. Sánchez-Martín, P.
535 Escobedo-Araque, S. Pernagallo, J.J. Díaz-Mochón, A colorimetric strategy based on
536 dynamic chemistry for direct detection of Trypanosomatid species, *Sci. Rep.* 9 (2019) 1–
537 13. <https://doi.org/10.1038/s41598-019-39946-0>.
- 538 [30] A. Robles-Remacho, M.A. Luque-González, R.A. González-Casín, M.V. Cano-Cortés,
539 F.J. Lopez-Delgado, J.J. Guardia-Monteagudo, M. Antonio Fara, R.M. Sánchez-Martín,
540 J.J. Díaz-Mochón, Development of a nanotechnology-based approach for capturing and
541 detecting nucleic acids by using flow cytometry, *Talanta*. 226 (2021).
542 <https://doi.org/10.1016/j.talanta.2021.122092>.
- 543 [31] S. Giunta, H. Funabiki, Integrity of the human centromere DNA repeats is protected by
544 CENP-A, CENP-C, and CENP-T, *Proc. Natl. Acad. Sci. U. S. A.* 114 (2017) 1928–1933.
545 <https://doi.org/10.1073/pnas.1615133114>.
- 546 [32] C. Chen, Y.K. Hong, S.D. Ontiveros, M. Egholm, W.M. Strauss, Single base
547 discrimination of CENP-B repeats on mouse and human chromosomes with PNA-FISH,
548 *Mamm. Genome*. 10 (1999) 13–18. <https://doi.org/10.1007/s003359900934>.
- 549 [33] ECACC General Cell Collection: HT29.
550 [https://www.culturecollections.org.uk/products/celllines/generalcell/detail.jsp?refId=910](https://www.culturecollections.org.uk/products/celllines/generalcell/detail.jsp?refId=91072201&collection=ecacc_gc)
551 [72201&collection=ecacc_gc](https://www.culturecollections.org.uk/products/celllines/generalcell/detail.jsp?refId=91072201&collection=ecacc_gc). Accessed 25 April, (2022).

- 552 [34] ECACC General Cell Collection: HeLa.
553 <https://www.culturecollections.org.uk/products/celllines/generalcell/detail.jsp?refId=930>
554 [21013&collection=ecacc_gc.](https://www.culturecollections.org.uk/products/celllines/generalcell/detail.jsp?refId=930) Accessed 25 April, (2022).
555 <https://www.culturecollections.org.uk/products/celllines/generalcell/detail.jsp?refId=930>
556 [21013&collection=ecacc_gc.](https://www.culturecollections.org.uk/products/celllines/generalcell/detail.jsp?refId=930)
- 557 [35] American Type Culture Colection (ATCC). MDA-MB-468 (htb-132).
558 <https://www.atcc.org/products/htb-132>. Accessed 28 Jan, (2022).
- 559 [36] J.H. Lee, E.R. Daugharthy, J. Scheiman, R. Kalhor, T.C. Ferrante, R. Terry, B.M.
560 Turczyk, J.L. Yang, H.S. Lee, J. Aach, K. Zhang, G.M. Church, Fluorescent in situ
561 sequencing (FISSEQ) of RNA for gene expression profiling in intact cells and tissues,
562 *Nat. Protoc.* 10 (2015) 442–458. <https://doi.org/10.1038/nprot.2014.191>.
- 563